CHAPTER 3

FINITE AMPLITUDE MOTIONS IN STABLY STRATIFIED FLUIDS

The previous chapter was based on equations of motion made linear by assuming that the amplitude of wave-like disturbances of the fluid remained infinitesimal. We now consider various large amplitude phenomena which require the inclusion of the non-linear terms for their explanation. First, some of the inviscid wave problems already treated will be extended to finite amplitude, and the essentially non-linear phenomenon of internal solitary waves will be discussed. Then various quasi-steady flows which arise in nature and in civil engineering applications will be treated, using a generalization of free surface hydraulic theory (and thus relating the properties of such flows to the waves which can form on them). Internal hydraulic jumps, the flow of a thin layer down a slope, and the nose at the front of a gravity current come under this heading. Finally we introduce the effects that viscosity and diffusion can have on slow steady motions in a stratified fluid, describing upstream wakes and boundary layers and the process of selective withdrawal.

3.1. Internal waves of finite amplitude

3.1.1. *Interfacial waves*

We refer again to the statement made in §2.1.2, that (2.1.8) is valid for finite amplitude long waves. (Cf. Lamb 1932, p. 278.) This implies that the highest point of any disturbance will move fastest, and so the forward slope of a wave of finite amplitude will tend to steepen, an effect called 'amplitude dispersion'. This is in contrast with the result of the frequency or wavenumber dispersion previously described by (2.1.7) which is valid for general depths. Since long waves propagate faster than short, this will lead to the spreading out of an arbitrary waveform and a decrease of slope. Thus it seems plausible that under some circumstances a balance between

these opposing tendencies can be achieved, and that it will be possible to have waves of finite amplitude and permanent form.

Some approximate results for internal waves of this kind will be quoted below. These are obtained by an expansion technique first used by Stokes for surface waves (and applied to interfacial waves by Hunt (1961)), and are given in the form of a power series in a small parameter, successive terms of which contain the higher harmonics. The first term represents the linear solution with sinusoidal waveform, and the higher order terms imply a distortion of this shape. One must be careful in each case to define the expansion parameter in such a way that it is indeed small. Initially it will be taken as the wave slope $(a_1 k)$ where a_1 is an amplitude and k the wavenumber, but in some later cases it will be seen that this needs modification, and the fluid depth must be taken into account. Thorpe (1968*a*, *c*) has made an extensive study, both theoretical and experimental, of progressive and standing waves at interfaces and in continuous stratification and his papers also contain a good survey of the earlier work. Other features of his experiment will be referred to in other chapters, but here only three special cases will be chosen for illustration and later use. All of these are for progressive waves on an interface, though comparable results were obtained for standing waves.

For two deep layers, the interface displacement η is given to third order by

$$\eta(x,t) = a_1 \cos(kx-\omega t) + \tfrac{1}{2} a_1 (a_1 k) \left(\frac{\rho_2-\rho_1}{\rho_1+\rho_2}\right) \cos 2(kx-\omega t)$$

$$+ a_1 \frac{(a_1 k)^2}{8} \frac{(3\rho_1^2 - 10\rho_1\rho_2 + 3\rho_2^2)}{(\rho_1+\rho_2)^2} \cos 3(kx-\omega t) \qquad (3.1.1)$$

and the dispersion relation is

$$\omega^2 = \frac{gk(\rho_2-\rho_1)}{\rho_1+\rho_2} \left\{ 1 + \frac{\rho_1^2+\rho_2^2}{(\rho_1+\rho_2)^2} (a_1 k)^2 \right\}. \qquad (3.1.2)$$

If the density difference is small, the distortion of the wave profile is determined by the third order term; this implies that the crests and troughs are symmetrical but flattened relative to a sine curve. The frequency for a given wavenumber increases with increasing amplitude.

When one layer is shallow (kh_1 small) and the other is deep, $(\rho_2-\rho_1) \ll \rho_2$, and T_1 denotes $\tanh kh_1$, then to second order

$$\eta(x,t) = a_1\cos(kx-\omega t) - \tfrac{3}{4}a_1(a_1k)\{(1-T_1)/T_1^2\}\cos 2(kx-\omega t) \tag{3.1.3}$$

and

$$\omega^2 = \frac{gk(\rho_2-\rho_1)T_1T_2}{\rho_1T_2+\rho_2T_1}\left\{1+\frac{(a_1k)^2}{8T_1}(9-22T_1+13T_1^2+4T_1^3)\right\}. \tag{3.1.4}$$

The form (3.1.3) shows that the wave profile is more sharply peaked on the side pointing into the deeper layer (and this result holds also for more general ratios of layer depths). This asymmetry has been observed in the laboratory and also in the ocean, as shown by the records obtained by La Fond (1966) in a shallow thermocline (reproduced in fig. 3.1). (Note however, that the whole picture is changed if there is a mean shear across the interface.)

For the third example we take that of equal layer depths, with at first an arbitrary density difference. Then with $h_1 = h_2 = h$, $T = \tanh kh$

$$\eta(x,t) = a_1\cos(kx-\omega t) + \tfrac{1}{4}a_1(a_1k)\left[\frac{(\rho_2-\rho_1)}{\rho_1+\rho_2}\frac{3-T^2}{T^3}\right]\cos 2(kx-\omega t) \tag{3.1.5}$$

and

$$\omega^2 = gkT\,\frac{(\rho_2-\rho_1)}{\rho_1+\rho_2}\left\{1+\frac{(a_1k)^2\,Y}{8T^4(\rho_1+\rho_2)^2}\right\},$$

where $$Y = [4(\rho_1+\rho_2)^2T^2(2T^2-1)+(\rho_2-\rho_1)^2(3-T^2)], \tag{3.1.6}$$

which in the case of small density differences simplifies to

$$\omega^2 = gkT\frac{(\rho_2-\rho_1)}{\rho_1+\rho_2}\left\{1+\frac{(a_1k)^2}{2T^2}(2T^2-1)\right\}. \tag{3.1.7}$$

When one or both of the layers is shallow, (3.1.4) and (3.1.7) show that there will be a reversal of the frequency dependence on wavelength at a particular depth, which for equal layers occurs at $T^2 = \frac{1}{2}$ or a depth to wavelength ratio of 0·140. The experiments of Keulegan and Carpenter (1961) show both that the frequency decreases with increasing amplitude for equal layers when they are

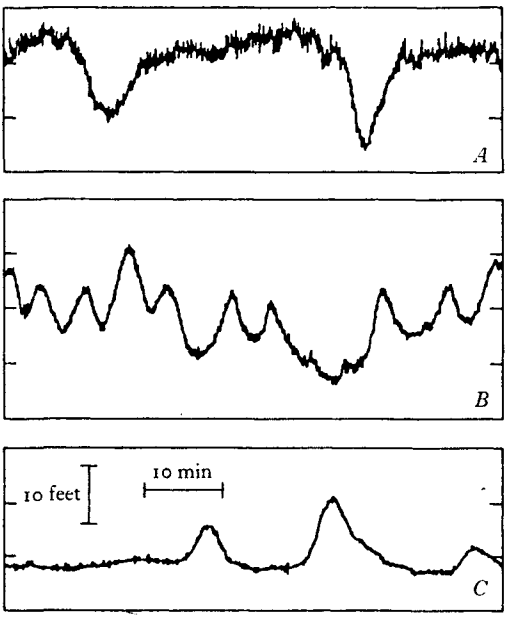

Fig. 3.1. Smoothed records of the shape of internal waves (A) near the sea surface, (B) at an intermediate depth and (C) near the sea floor. (From La Fond 1966. In *Encyclopedia of Oceanography*, ed. R. W. Fairbridge, © 1966 by Litton Educational Publishing, Inc. Reprinted by permission of Van Nostrand Reinhold Company.)

shallow enough, and that the wave profiles are symmetrical and very nearly sinusoidal, in agreement with (3.1.5).

Another consequence of a finite amplitude wave motion at an interface, i.e. the retention of second order terms, is that the orbits of individual fluid particles are changed. A steady horizontal drift in the direction of wave propagation, of order $(a_1 k)^2$, is superimposed on the circular orbits, with a maximum at the interface and an exponential decay on each side (cf. the 'Stokes drift' for surface waves). As Dore (1970) has shown, a small viscosity greatly increases this effect, producing a current proportional to $(a_1 k)^2 Re^{\frac{1}{2}}$, where $Re = (\omega/\nu k^2)$ is a Reynolds number based on the wave motion. The calculated form of the velocity profile in a channel with rigid top and bottom is shown in fig. 3.2. The conditions of no net horizontal flow imposed on this solution is appropriate to the case of a tank of limited length, and measurements of the distortion of dye

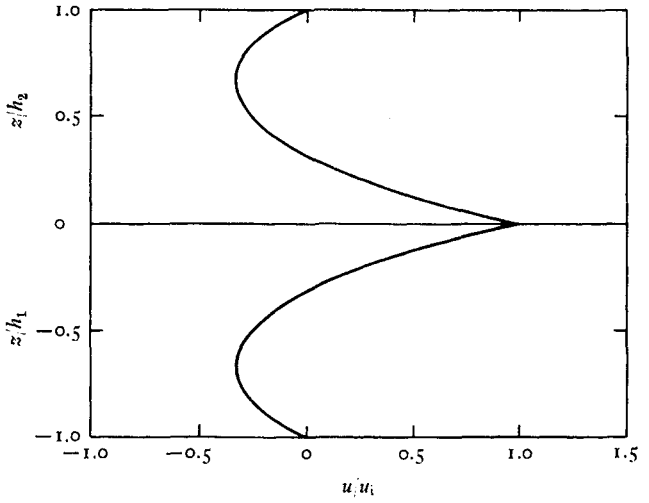

Fig. 3.2. The profile of horizontal mass transport velocity for a progressive wave moving from left to right in a two-layer fluid system bounded by two rigid horizontal planes. (After Dore 1970.)

streaks show the same general features. When the interface is not sharp, however, a backflow is predicted near the centre, and there is the extra complication that the density distribution is distorted near the ends of the tank and the simple drift cannot continue indefinitely. Similar drift motions have been documented by Thorpe (1968*c*) for the case of continuous stratification.

3.1.2. *Cnoidal and solitary waves*

It is clear that when one or both of the layer depths is small enough for $\tanh kh \approx kh$ to be small, the above expansions must become invalid. In this limit, the ratio of the coefficient of the second harmonic in (3.1.5) to that of the first is of order

$$\frac{a_1}{k^2h^3}\frac{\rho_2-\rho_1}{\rho_1+\rho_2} = l_1 \tag{3.1.8}$$

which need not be small just because a_1k is small. A different procedure is necessary when both layers are shallow which in effect uses l_1 as the expansion parameter, and puts a limitation on its magnitude. Similarly, the ratio of the corresponding coefficients in (3.1.3) is of order

$$a_1/kh_1^2 = l_2, \tag{3.1.9}$$

and this is the appropiate parameter to use when only one layer is thin. The difference between l_1 and l_2 is of some importance, which will be brought out in the discussion below.

For the case of two thin layers Benjamin (1966) has obtained valid solutions for periodic waves of permanent form (called cnoidal waves because of the symbol 'cn' used to denote the Jacobian elliptic functions which describe their shape). He used a method which takes no account of the fact that the density difference in l_1 may be small, i.e. it does not rely on the Boussinesq approximation. We will write down explicitly only the result for the limiting case as $kh \to 0$, that is, for the internal solitary wave (first considered by Keulegan (1953)). The interface displacement from its state of rest can be written, neglecting terms of order $(a_1/h)^4$, as

$$\eta = a_1 \operatorname{sech}^2 \frac{x}{2b}, \tag{3.1.10}$$

where the lengthscale b depends on the densities and layer depths. With equal layers and rigid boundaries, for example, the displacement is upwards and

$$b^2 = \frac{1}{3} \frac{h^3 \rho_1 + \rho_2}{a_1 \rho_2 - \rho_1} \left\{ 1 + \frac{a_1}{h} \frac{\rho_2 - \rho_1}{\rho_1 + \rho_2} \right\}. \tag{3.1.11}$$

For unequal layers and small density differences the crest of the wave is towards the deeper layer. If b is identified with the wavelength k^{-1} in (3.1.8) it is clear that the parameter l_1 is of order unity for internal solitary waves. The longer the wave, the smaller must be its amplitude for the required balance between the two non-linear effects to be maintained; higher waves will continue to steepen and even break (see §3.2.2). The phase velocity is

$$c^2 = gh \frac{(\rho_2 - \rho_1)}{(\rho_1 + \rho_2)} \left[1 + \frac{\rho_2 - \rho_1}{\rho_1 + \rho_2} \frac{a_1}{h} \right], \tag{3.1.12}$$

always greater than that of infinitesimal waves; the solitary wave is in fact the fastest travelling wave of given height and unchanging form.

Analogous results have been obtained by Long (1965) and Benjamin (1966) for solitary waves in a continuous (exponential) density gradient. They showed that in that case it is not possible to use the Boussinesq approximation since this implies an inconsistent

neglect of terms which may be of the same order as others which have been retained. A crude indication of what can happen is obtained by examining (3.1.6) (and a similar coefficient in the next term omitted from the expansion (3.1.5)). When T is small, the two terms in the factor Y are generally comparable, and though they are small, an accurate estimate of both of them is essential when discussing the limit corresponding to the solitary wave.

A different kind of internal wave can exist on a thin layer of light fluid lying over a deep layer, or in the equivalent circumstances described below. Benjamin (1967) has produced a comprehensive theory for progressive waves and continuous variations of density confined to shallow regions, but again only the solitary wave solution on uniform layers between rigid boundaries will be written down here. The interface displacement is downwards, and provided a_1/h_1 is fairly small, is of the form

$$\eta = \frac{-a_1\lambda^2}{x^2+\lambda^2}, \tag{3.1.13}$$

where

$$\lambda = \frac{4\rho_1}{3\rho_2}\frac{h_1^2}{a_1}.$$

This is clearly consistent with l_2 (defined by (3.1.9)) being of order unity if λ^{-1} is identified with k. The phase velocity is

$$c^2 = \frac{\rho_2-\rho_1}{\rho_1}g(h_1+\tfrac{3}{4}a_1); \tag{3.1.14}$$

note the much stronger dependence on amplitude than in (3.1.12), when the density difference is small. A free surface has the effect of decreasing both the speed and the length of the wave, for a given amplitude.

Solitary waves of this second type are likely to be important on the seasonal thermocline i.e. below a thin light layer at the surface of the ocean. They can also occur on a thin transition region between two uniform layers, and then (by symmetry) take the form of bulges travelling along the interface. They were first observed in the laboratory by Davis and Acrivos (1967*a*) in a study which brought out the close relationship between these bulges and the second mode waves formed as a result of resonant interactions (see fig. 2.18). It was shown that such a disturbance can propagate back and forth along a tank, being reflected off the ends and persisting until

damped by viscosity (fig. 3.3*a* pl. III). The measured velocities were in good agreement with an expression equivalent to (3.1.14), modified to take account of the actual density distribution. When the amplitude of the disturbance is larger, the character of the motion changes, and a lump of fluid having a circulation like that in a vortex pair propagates bodily along the interface (fig. 3.3*b*). Davis and Acrivos produced numerical calculations, valid for large amplitude, which contain this feature of closed streamlines (though the equations themselves break down in this range for another reason, which will be discussed in §3.1.3).

3.1.3. *Waves and flows in a density gradient*

As mentioned above, related expansion techniques have been used to calculate the form of internal waves with continuous stratification (for example by Thorpe (1968*c*) and Benjamin (1966)) but these problems will not be pursued further here. We turn instead to a restricted class of flows for which exact solutions can be obtained, but with no limitation on amplitude (such as is still required by (3.1.8) and (3.1.9)). Dubreil-Jacotin (1937) and Long (1953*a*) derived an exact first integral of the equations of motion which is in general non-linear, but which becomes linear (without approximation) for special choices of stratification and velocity. Much of the detailed work on large amplitude waves has been based on this simplification.

Several forms of this equation will be written down below without proof, but the conditions necessary for their validity must be clearly understood. The motion is supposed two-dimensional, incompressible and steady. At some horizontal position upstream of the body (in the negative x-direction) there are no disturbances and the velocity and density distributions are specified functions of z. Finally, there should be no reversal of flow in any vertical section, so that a streamfunction ψ may be defined which varies monotonically with z, and the density $\rho = \rho(\psi)$ (i.e. is constant along streamlines). With these assumptions (which will be discussed further below) it follows from the full inviscid equations of motion that

$$\nabla^2\psi + \frac{1}{\rho}\frac{\mathrm{d}\rho}{\mathrm{d}\psi}\left[\tfrac{1}{2}(u^2+w^2)+gz\right] = f(\psi), \qquad (3.1.15)$$

where $$u = \partial\psi/\partial z, \quad w = -\partial\psi/\partial x$$

and $f(\psi)$ is a specified function of ψ.

Yih (1960) gave a transformed version of (3.1.15) in terms of a pseudo-streamfunction $\tilde{\psi}$ defined by

$$\rho^{\frac{1}{2}}u = \partial\tilde{\psi}/\partial z, \quad \rho^{\frac{1}{2}}w = -\partial\tilde{\psi}/\partial x$$

(whose definition is related to the procedure discussed at the end of § 1.3, which removes the inertia effects). This may be written

$$\nabla^2\tilde{\psi} + gz\frac{\mathrm{d}\rho}{\mathrm{d}\tilde{\psi}} = \frac{\mathrm{d}H_*}{\mathrm{d}\tilde{\psi}}, \tag{3.1.16}$$

where $H_* = p + \frac{1}{2}(u^2+w^2) + g\rho z$ is the 'total head', which is constant along a streamline. From this form it is clear that the equation is linear provided both ρ and H_* are polynomials of degree no higher than quadratic in $\tilde{\psi}$. Yih (1965) has discussed the various possible cases, one of which corresponds to the situation of interest here. If both $\mathrm{d}\rho/\mathrm{d}z$, the density gradient, and $\frac{1}{2}\rho U^2$, the dynamic pressure, are assumed independent of z in the undisturbed flow, (3.1.16) reduces to an especially simple form. At the same time one can introduce the displacement η_0 of the streamlines from their initial position as the dependent variable, to obtain the equation which is our starting point in the following section on lee waves

$$\nabla^2\eta_0 + \frac{N^2}{U^2}\eta_0 = 0. \tag{3.1.17}$$

Note that the Boussinesq assumption has not yet been made, but when it is added, the condition on (3.1.17) is that N^2 and U^2 separately should be constant with height. This equation, with constant coefficients, is the Helmholtz equation, exactly the same form as that obtained for $(\partial^2 w/\partial x^2)$ in the linear theory (2.3.1).

The assumptions leading to (3.1.17) can break down in several ways. Most important in the lee wave application is the restriction that all streamlines must emanate from a position far upstream. It will be shown in § 3.1.4 that statically unstable regions with closed streamlines appear in the solutions when the wave amplitude becomes large; though such 'rotors' are physically plausible, they cannot consistently be described using the present model. There is also the problem of 'upstream influence', the possibility that the

introduction of a finite obstacle into a flow on which lee waves can form will result in 'columnar' disturbances extending upstream (i.e. those having $k = 0$; see §2.3.1). From the first of equations (2.2.11), it is clear that energy could then propagate upstream provided the vertical wavenumber $m < N/U$; if such motions were present they would change the approaching flow and thus violate the assumed conditions far upstream.

The columnar disturbances are not needed to satisfy the boundary conditions in the lee wave problem, but they can nevertheless arise in connection with non-linear transient effects. Benjamin (1970) gave an integral argument concerning the inviscid transient problem which suggested that there will always in principle be an upstream influence in a confined flow which is subcritical in the sense used in §2.3.1. McIntyre (1972) has modified this conclusion by showing that, while there will always be a columnar disturbance, this need not appear ahead of the body. For the first lee wave mode there is an upstream influence (to second order in the wave slope) only when $NH/U > 2\pi$, i.e. under conditions where a second mode can also appear. Though the question has a basic philosophical importance, it is often of less practical significance. Even when upstream influence is predicted it is weak, and it is still useful in practice to investigate the effects of an obstacle for a given flow upstream, disregarding the changes in the flow caused by the introduction of the obstacle. In an unconfined flow the disturbances fall off with distance, and the assumption of no upstream influence is formally valid at large times after the introduction of the obstacle (though of course disturbances could arise in other ways not considered here, for example through the mechanism of resonant interaction described in §2.4.3).

An associated difficulty raised by Benjamin (1966) has not yet been fully resolved. He has questioned whether the special boundary conditions imposed to bring the equations to linear form are in fact representative of the full non-linear steady problem (which requires also the specification of a downstream boundary condition). Certainly the 'critical layer' phenomena of §2.3.3, as well as the formation of the rotors mentioned above and of hydraulic jumps (§3.2.2) are excluded from the formulation based on the assumptions leading to (3.1.17).

3.1.4. *Finite amplitude lee waves*

Because of the identical form of (2.3.1) and (3.1.17) the solution to some non-linear problems can be obtained directly from the linearized solutions described in §2.3. The boundary condition at the obstacle is still essentially non-linear, however, since the lowest streamline must follow its surface, which may have an arbitrary height. Long (1955) showed (for the case of a closed channel) how an *inverse* method can be used to calculate related flowpatterns and obstacle shapes. He first calculated streamlines for a convenient shape of infinitesimal barrier, using a superposition of linear solutions, and then increased the amplitude of the motion to a finite value. The resulting solution still satisfies (3.1.17) but it no longer satisfies the boundary conditions on the obstacle (which on the linearized theory were applied at $z = 0$). The final step is to replace the original obstacle by another having the shape of the bottom streamline calculated in this way, on which the conditions are automatically satisfied.

Long (1955) compared his calculated streamlines for various obstacle shapes and heights with flow patterns observed in a series of laboratory experiments (which remain the best and most comprehensive in this field). All his photographs are worth detailed study, but only two are reproduced here. In fig. 3.4*a*, *b* pl. v are compared the observations and calculations in a case where only one lee wave mode can occur, and fig. 3.4*c*, *d* correspond to the range with lower velocity ($Ri_0^{\frac{1}{2}} > 2\pi$) where a second mode appears. In the second case rotors are observed, but apart from the fact that the observed wave motions are weaker than predicted, the agreement between theory and experiment is surprisingly good, and the flow outside these regions of reversed flow is apparently little affected by their presence. Some alteration of the flow ahead of the obstacle is also seen in fig. 3.4*d*, a first indication of the 'blocking' which becomes important in very slow flows or for high barriers. (This phenomenon is discussed further in §§3.2.1 and 3.3.2. Note that it is a different limiting case from that described earlier in connection with 'upstream influence', when flows of finite velocity over small barriers were of interest.)

Yih (1960) used a different inverse approach, in which instead of

specifying a barrier shape he investigated (using a linearized form of (3.1.16)) the effect of introducing various singularities into a stratified flow in a channel. A vertical line of cross-stream vorticity, for example, can produce a region of closed streamlines in its neighbourhood, as well as wave-like disturbances downstream. By choosing the boundary of this closed region as the shape of the obstacle, one again obtains a possible exact solution for the flow over a rather blunt body. Source and sink distributions (with total strength zero) can also be used, a device closely analogous to that used by Rankine to generate streamlined bodies in a uniform inviscid flow. Pao (1969) has extended Yih's method by using distributions of vortex pairs and doublets to generate barriers and satisfy upstream boundary conditions in a semi-infinite as well as a confined flow. (Again these calculations were continued well past the point where the equations no longer give a valid description of the flow.)

One more result for channel flows should be mentioned. Claus (1964) used a comparable equation to (3.1.17) for a compressible flow, and calculated exact lee wave patterns for particular density and velocity distributions using Long's method. He then compared this with a similar calculation for an incompressible fluid having the same velocity profile but a density stratification the same as the potential density distribution in the compressible flow. The wavelengths in the case compared were identical, but the maximum amplitude in the compressible case was nearly twice that of the incompressible flow, reflecting the fact that it is density and not potential density which determines the energy density.

When indirect methods are used, the shape of a barrier producing waves cannot be specified *a priori*. It is much more convenient to be able to fix the shape, and then investigate systematically what happens to the lee waves as the stratification and flow velocity are changed. Drazin and Moore (1967) were the first to obtain such a solution, with boundary conditions prescribed on a thin vertical strip projecting above the floor of a channel. Important as this solution was theoretically, it is an unrealistic case physically (because the flow cannot remain attached to such a barrier – see below). A series of papers by Miles (1968*a*, *b*)† and Miles and Huppert (1969) has shown how a modified diffraction theory, familiar in

† Miles (1969) has also given an excellent review of the whole subject.

other contexts, can be used to solve the problem for any obstacle shape in a closed channel and for an infinite half-plane. Only the latter will be considered here; for this case, we recall, it can be shown that there will be no 'upstream influence' extending to $x = -\infty$.

The governing equation (3.1.17), obtained by making the assumptions $\mathrm{d}\rho/\mathrm{d}z = \text{const}$ and $\rho U^2 = \text{const}$, can be written in the non-dimensional form

$$\nabla_1^2 \eta + \kappa^2 \eta = 0, \tag{3.1.18}$$

where both $\eta = \eta_0/h$ and the dimensionless operator ∇_1^2 are scaled with the maximum height h of the barrier, and $\kappa^2 = (Nh/U)^2$ has the form of an overall Richardson number. The lee waves depend on the *obstacle* height through the parameter κ^2, which is different from the Ri_0 used to characterize the whole flow in §2.3.1. Ri_0 is always large since a lengthscale $H \gg h$ comparable with the scale height of the whole region of interest must be used. The range of interest of the constant κ is roughly $0 < \kappa < 1.5$, as the barrier height for a given flow is increased from zero to that at which the flow becomes unstable, in the sense that overturning and backflow first appears. At this point, when $\kappa = \kappa_c$, a streamline becomes vertical somewhere in the flow and the model is strictly invalid at larger κ, though outside the regions of overturning the solutions again seem to describe observed phenomena reasonably well. Another kind of instability, which draws energy from the shear flow due to the waves, will be discussed in chapter 4.

Streamlines calculated by Huppert for the case of a semi-circular obstacle are shown in fig. 3.5, for three values of κ: $\kappa = \kappa_c = 1.27$ and two values on either side of this. The increase of amplitude of the waves and the tendency to overturn as κ is increased are clearly seen. Values of κ_c have also been calculated for a wide variety of obstacle shapes, using a representation in terms of appropriate distributions of dipole sources (cf. the indirect methods). Given the functional form, two parameters are enough to specify the shape, namely κ and $\epsilon = h/b$ where b is a measure of the width. Huppert and Miles (1969) explored the whole range of semi-elliptical obstacles, for which κ_c varies smoothly from 1.73 for $\epsilon = \infty$ (corresponding to the vertical strip) through $\kappa_c = 1.27$ at $\epsilon = 1$ (the semi-

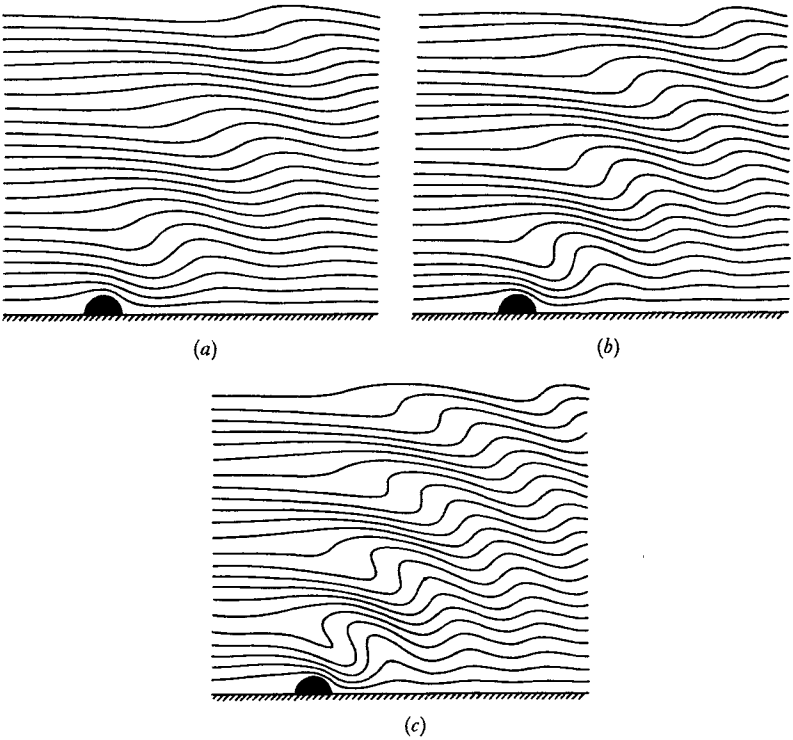

Fig. 3.5. Streamlines of a stratified flow over a semi-circular obstacle, calculated by Huppert (1968) using (3.1.18) (*a*) $\kappa = 1.0$, (*b*) $\kappa = \kappa_c = 1.27$, (*c*) $\kappa = 1.5$.

circle), to 0·67 at $\epsilon = 0$. In the last paper of the series they investigated various limiting cases and compared them with the exact solutions. When $\kappa \to 0$ with ϵ fixed (i.e. weak waves are formed behind a body of *given shape*) a simple dipole field results, with amplitude proportional to the moment of the dipole, and therefore to the cross-sectional area of the obstacle hb (as remarked in §2.3.1). The limiting solutions as $\epsilon \to 0$ with κ/ϵ fixed (i.e. for a *fixed length* of obstacle) show that the linear theory is accurate only for $\kappa \ll 1$. The largest value of κ_c ever found explicitly for a wide flat body is $\kappa_c = 0{\cdot}85$, for the shape $z = h[1+(x/b)^2]^{-1}$ used in so many linear lee wave computations (see §2.3.2).

The direct calculations of Miles and Huppert also lead to numerical estimates of the drag coefficient (for the limited class of

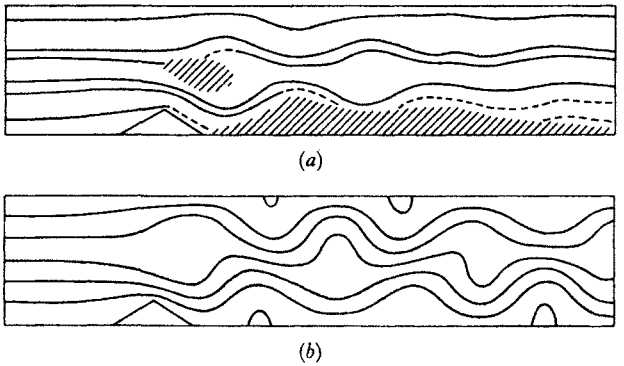

Fig. 3.6. Flow over a triangular obstacle with $\kappa = 2.7$. (From Davis 1969.) (*a*) observed flow, with hatched areas denoting mixing regions; (*b*) calculated flow, showing rotors.

flows described by (3.1.18); reference should again be made here to the work of Benjamin (1970) who has shown that the drag exerted by an obstacle on a stream is intimately connected with the question of upstream influence). A knowledge of the flow pattern immediately allows a computation of the change in the flux of horizontal momentum, and hence of the wave drag D. The drag coefficient C_D is defined by comparing D to the force due to the dynamic pressure $p_1 = \frac{1}{2}\rho U^2$ acting over the height h of the body, so

$$C_D = D/p_1 h. \tag{3.1.19}$$

The drag coefficient for tall ellipses is a monotonically increasing function of κ at any ϵ, which varies little with ϵ, whereas for squat ellipses it depends more strongly on ϵ as well as on κ. For all elliptical bodies, however, the maximum C_D for unseparated flows with $\kappa < \kappa_c$ varies little, between 2·3 at $\epsilon = \infty$ to 3.0 at $\epsilon = 0$. A comparison of the exact C_D with the drag calculated using the several asymptotic approximations of Miles and Huppert (1969) referred to above showed that there is a substantial range of κ/ϵ where only the full solution gives an accurate estimate of C_D.

Davis (1969) has used a related method to obtain numerical solutions for the flow over a triangular obstacle in a channel of finite depth. He has also compared his solutions with laboratory experiments which are especially interesting in that they emphasize the differences between the assumed and actual flows for the same

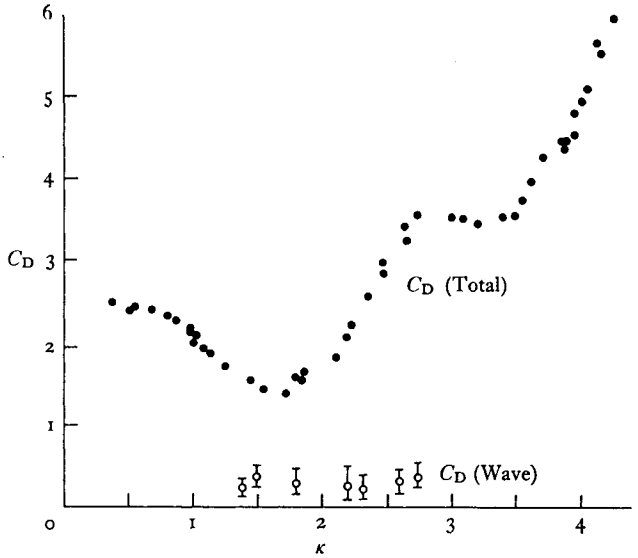

Fig. 3.7. Comparison between measured total drag and wave drag coefficients for a stratified flow over a thin barrier. (After Davis 1969.)

nominal upstream conditions. Using triangular and also thin barriers, he recorded flowpatterns (fig. 3.6) which are a combination of a turbulent wake due to the separation of the flow from the sharp-edged bodies, lee waves produced by the barrier and the wake, and also the turbulent rotors which form as a result of the waves but are not adequately dealt with by the theories based on (3.1.18). He made an estimate of the pure wave drag from the observed amplitude of the waves, and compared this with direct measurements of drag, made by towing a floating obstacle along the channel and measuring the force on it. As shown in fig. 3.7, the total drag is considerably greater than the wave drag, and this must be due to phenomena which are not described by lee wave theory. Outside the 'stable' range of $\kappa < \kappa_c$, the wave solutions provide no guide at all to the behaviour of the flow or to the drag. (The properties of the turbulent wake as such will be discussed further in §5.3.1.)

3.2. Internal hydraulics and related problems

The flow of a layer of heavy fluid under lighter fluid has many features in common with the hydraulics of a stream with a free surface. Some of these analogous properties will now be summarized, as a prelude to the discussion of the new effects which become possible when the density differences are small and the fluids can mix freely. In nature, most flows of this kind are turbulent, but they can for many purposes be accurately described using perfect fluid theory, with sometimes the addition of terms to take into account friction on the bottom and at the interface, and the overall energy losses.

3.2.1. *Steady frictionless flow of a thin layer*

Consider first a two layer system in two dimensions, with a layer of depth $h_1(x)$, density ρ_1 flowing with a velocity U in the x-direction under a deep layer at rest. Suppose that an obstacle is introduced, with height $h = h(x)$ above the horizontal bottom, and length $L \gg h$ so that the flow is slowly varying and can be regarded as uniform at any section. Applying Bernoulli's equation just below the interface gives

$$\frac{p_1}{\rho_1} + \tfrac{1}{2}U^2 + g(h+h_1) = \text{const}, \tag{3.2.1}$$

where p_1 is the pressure at the interface, and just above:

$$\frac{p_1}{\rho_2} + g(h+h_1) = \text{const} \tag{3.2.2}$$

(any change in velocity in the upper layer will be small because its depth is large). The continuity equation in the lower layer is

$$Uh_1 = Q \quad \text{say}, \tag{3.2.3}$$

and eliminating p_1 and U from the above gives

$$\frac{1}{2g'}\frac{Q^2}{h_1^2(x)} + h_1(x) = C - h(x), \tag{3.2.4}$$

where C is a constant. This is of exactly the same form as the ordinary hydraulic relation with $g' = g(\rho_1 - \rho_2)/\rho_1$ replacing g, and is sketched in fig. 3.8.

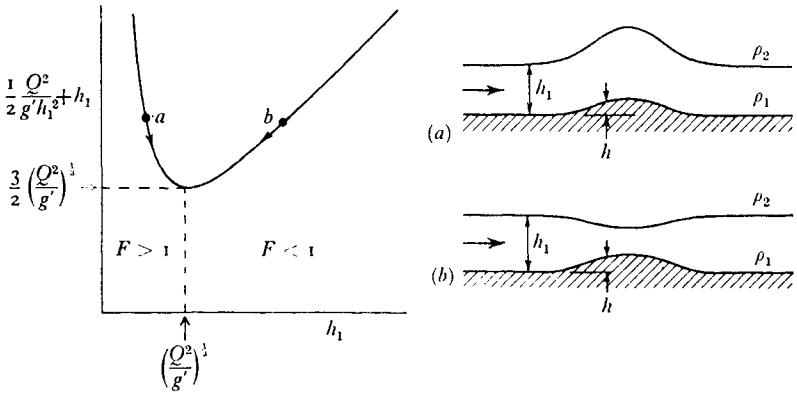

Fig. 3.8. The behaviour of a heavy layer flowing over an obstacle and under a deep lighter layer at rest, as described by the 'hydraulic' relation (3.2.4). If the flow is supercritical upstream, (situation (*a*) $F > 1$) the interface bows upwards over the obstacle; if it is subcritical (as at (*b*) with $F < 1$) the interface drops.

Given the form of the obstacle $h(x)$ the volume flux per unit width Q and the constant C, the depth of the layer h_1 can be found from (3.2.4). Its behaviour depends critically on the upstream value of the internal Froude number defined by (cf. (1.4.5))

$$F = \left(\frac{Q^2}{g'h_1^3}\right)^{\frac{1}{2}} = \frac{U}{(g'h_1)^{\frac{1}{2}}},$$

since the left-hand side of (3.2.4) has a minimum at $F = 1$. If $F > 1$ far upstream, h_1 will increase as $h(x)$ increases and the interface bows upwards over the obstacle (as shown in fig. 3.8*a*). If $F < 1$ on the other hand, the level drops ($h + h_1$ decreases) as the flow draws on its potential energy to gain enough kinetic energy to surmount the obstacle (fig. 3.8*b*).

The 'critical' internal Froude number $F = 1$ corresponds to the state in which the flow velocity just equals the velocity of *infinitesimal* long waves on the layer, called the critical velocity U_c. (See (2.1.8).) When the flow is supercritical ($F > 1$), small disturbances cannot propagate upstream against the flow and any obstacle will have a purely local effect. When the flow is subcritical ($F < 1$), short waves can remain at rest relative to the obstacle, and so a phenomenon analogous to lee waves on the interface can be observed downstream of shorter obstacles (Long 1954). (This criterion

for wave formation can be compared with that found in §2.3.1 for a continuous gradient, namely $F = Ri_0^{-\frac{1}{2}} < \pi^{-1}$, remembering of course the different definition of the internal Froude number.)

This subcritical case also sheds some light on the difference between the phenomena of upstream influence and blocking. In general, when stationary waves appear downstream, longer waves can propagate upstream, but if h is small these will be damped by friction. Though there is undoubtedly an upstream effect, its net result is small. If h is increased beyond the point where the right-hand side of (3.2.4) falls below $\frac{3}{2}(Q^2/g')^{\frac{1}{3}}$, however, no solution is possible, essentially because the fluid no longer has enough energy to get over the barrier. In this case true blocking occurs, and the depth upstream must increase until a new steady state is established with $F = 1$ over the obstacle, which now acts as a control section for the whole flow. Upstream the flow is subcritical, with depth h_0 say, and above the obstacle (where the depth is $\frac{2}{3}h_0 = h_c$, the critical depth) it changes smoothly to a supercritical flow downstream.

3.2.2. *Internal hydraulic jumps*

Changes in the flow can also take place more abruptly. For example, when the blocking described above is produced by suddenly increasing the height of an obstacle, the front of the layer of increased depth may be very sharp, and will propagate upstream as a travelling hydraulic jump (also called a bore or surge). If the supercritical flow below the barrier is obstructed again further downstream, it can pass again into a subcritical flow through a stationary hydraulic jump (fig. 3.9). This arises as a result of finite amplitude long waves, which can travel faster than U_c and therefore move upstream, transmitting information faster than is possible on linear theory. (Such waves, whose properties depend only on the local mass flux and the continuity equation have been called 'kinematic waves' by Lighthill and Whitham 1955.) If their amplitude becomes so large that frequency dispersion can no longer balance the steepening effect (see §3.1.2), then the upstream face of the wave eventually breaks, with the accompanying turbulence which characterizes jumps and surges.

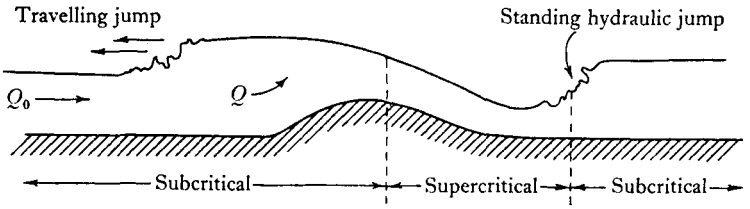

Fig. 3.9. Flow of a layer over a high obstacle: production of internal hydraulic jumps.

The conditions at a jump can be investigated using the conservation of momentum and mass, i.e. by applying (3.2.1) and (3.2.3) to the states before and after the jump where the depths are h_1 and h_1'. It follows on eliminating the velocities that

$$h_c^3 = \tfrac{1}{2}h_1 h_1'(h_1 + h_1'); \tag{3.2.5}$$

thus a stationary jump can only occur between two 'conjugate' states, one shallower and the other deeper than the critical depth. The final depth h_1' may be expressed in terms of h_1 and F_1 upstream as

$$h_1' = \tfrac{1}{2}h_1[(1 + 8F_1^2)^{\frac{1}{2}} - 1]. \tag{3.2.6}$$

By comparing the fluxes of kinetic energy before and after a jump, it can be shown that a jump can only take place from a supercritical to a subcritical flow, and that an amount of energy equal to

$$\frac{(h_1' - h_1)^3 g' Q}{4h_1 h_1'} \quad \text{per unit span}$$

is dissipated in the process. (The opposite case would imply a creation of energy at the jump.) When F_1 is only just supercritical (a weak jump), some of the energy can be radiated away in the form of internal waves, but at higher F_1 not enough energy can be dissipated in the waves alone and they must break (Benjamin 1966, 1967). In strong jumps little energy goes into waves.

Phenomena which can be interpreted in terms of each of these processes have often been observed in the atmosphere (Ellison 1961). A sudden pressure change, accompanied by a change in wind speed, can signal the passage of a strong jump. Regular oscillations

in a barometer record (with the number of crests increasing in time as the energy travels away from the jump) correspond to an undulating jump. Sometimes condensation and precipitation effects complicate and intensify the atmospheric jump phenomenon (producing a 'squall line'); the same is true if a moist supercritical flow passes over a mountain, where the thickening and lifting can give rise to heavy orographic rainfall. Other related processes which are important in the atmosphere, but which do not have close parallels in ordinary hydraulic theory, remain to be discussed in later chapters, namely the effect of a continuously stratified environment above the flowing layer (§9.2) and the turbulent mixing produced by the kinetic energy released in a jump (§6.2.3).

The above ideas have been generalized to apply to several layers having arbitrary depths and velocities, notably by Long (1954). He concentrated on the case of comparable depths and equal velocities, simulating this experimentally by moving an obstacle through a tank containing immiscible layers, initially at rest. He produced convincing demonstrations of the various regimes of flow over the obstacle, and of the jump phenomena (fig. 3.10 pl. v), and applied the ideas (Long 1953*b*) to explain the violent winds and turbulence observed in the flow over the Sierra Nevada range (see fig. 3.11 pl. vi). More recent developments in this field, which will also be important in the study of changing flows in shallow estuaries, have been summarized by Yih (1965, p. 130), and reference has already been made to the observations by Thorpe *et al.* (1972) of large amplitude internal seiches in a lake, which take the form of surges travelling along the thermocline and reflecting from the ends.

3.2.3. *Flow down a slope*

In considering changes in the flow along a horizontal bed which take place over a relatively short distance, it was reasonable to neglect friction as we did above; but when the flow of a heavy layer down a long slope is of interest, friction must certainly be added if the velocity is not to increase without limit. Here, following the usual hydraulic assumption, we take the drag to be proportional to the square of the velocity and to include the effects of friction at the bottom and at the interface. (The form of the latter is treated more

fully in § 6.2.) The momentum equation parallel to a slope at a small angle θ to the horizontal is then

$$\frac{\mathrm{d}}{\mathrm{d}x}(U^2 h_1) = g' h_1 \theta - g' h_1 \frac{\mathrm{d}h_1}{\mathrm{d}x} - C_\mathrm{D} U^2, \tag{3.2.7}$$

where the terms on the right represent respectively the component of gravity accelerating the layer, the pressure force due to a possible change in depth, and the frictional force (C_D now being used to denote a combined drag coefficient). Eliminating the velocity using (3.2.3) gives

$$\frac{\mathrm{d}h_1}{\mathrm{d}x}(1 - F^2) = (\theta - C_\mathrm{D} F^2). \tag{3.2.8}$$

When $F = 1$ (and $h_1 = h_\mathrm{c}$, the critical depth), $\theta = C_\mathrm{D}$, the critical slope; a smooth change from subcritical to supercritical flow or vice versa can only occur when the slope is critical. More generally, when the flow is uniform and $\mathrm{d}h_1/\mathrm{d}x = 0$, $F^2 = \theta/C_\mathrm{D}$, a constant which depends only on the slope and the friction, not at all on the rate of supply of fluid or its density. The corresponding *normal depth* of the flow h_n is from the equation on p. 65

$$h_\mathrm{n}^3 = C_\mathrm{D} Q^2/\theta g'. \tag{3.2.9}$$

When a flow is started with depth $h_0 \neq h_\mathrm{n}$ its behaviour depends on the relative magnitudes of h_0, h_n and h_c. If $h_0 > h_\mathrm{n} > h_\mathrm{c}$, $\mathrm{d}h_1/\mathrm{d}x$ is positive and tends towards θ for large x; this flow can remain subcritical everywhere and spread out smoothly to merge with a layer of heavy fluid overlying a horizontal plane at the bottom of the slope (see fig. 3.12). Supercritical flows, on the other hand, can only change to subcritical through a jump, which may occur either on the slope or further out over the horizontal plane. An especially convincing application of this result was made by Ball (1957). He explained the sudden changes from light to strong winds at a coastal station in Antarctica in terms of the movement of a jump, which is formed as the katabatic wind (the downslope flow formed by cooling of the air over the continent) flows over the sea. Sometimes it is not clear if one should describe observations in these terms, or as a flow over an obstacle (fig. 3.9); the important feature in either case is that the flow is supercritical at the slope. Although a line of clouds, strong rotary motions and sometimes waves downstream are associated

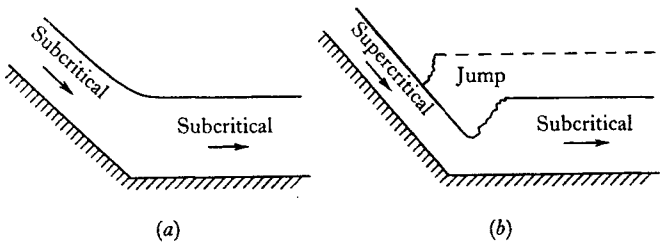

Fig. 3.12. Flow of a heavy layer down a slope and onto a horizontal plane (*a*) a subcritical flow can spread out smoothly, (*b*) a supercritical flow must become subcritical through a hydraulic jump, whose position can change as the flow rate fluctuates.

with such hydraulic jumps, they arise in a rather different way from ordinary 'lee waves' and the rotors discussed previously, which can only be formed when the flow over a mountain is subcritical.

3.2.4. *The 'lock exchange' problem*

We turn now to phenomena in which the intrusion of a front or 'nose' into a fluid of different density is the main concern, rather than the steady flow of the layer behind it. Important examples are the motion of a front of cold air under warmer air in the atmosphere (on a small enough scale for rotation to be neglected, say a sea-breeze front rather than one associated with a large depression), or the intrusion of salt water under fresh when a lock gate is opened at the mouth of a river. Following Benjamin (1968) we will concentrate here on flows along a horizontal plane. It has been shown by Middleton (1966) that for small slopes the motion of the nose can be described using the depth and density difference at the nose itself, with the slope and the depth of the layer behind playing only a secondary role. (See the next section and especially §6.3.4 for a discussion of noses on steep slopes.)

Consider first a two-dimensional frictionless flow in a closed channel of depth d, referred to axes fixed relative to the nose (see fig. 3.13 for the notation). As in §3.2.1, continuity and Bernoulli's equation applied just above the interface give two equations involving the final velocity U_2 and depth h of the flowing layer. In the absence of friction a third relation follows from the fact that the

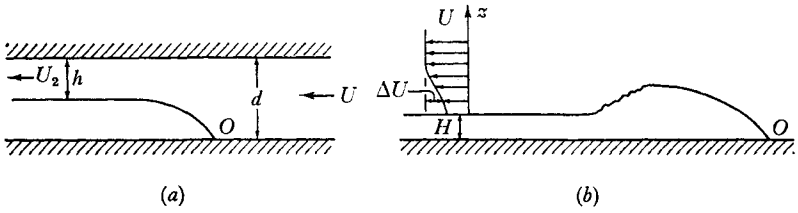

Fig. 3.13. Two-dimensional flow of a heavy layer. (*a*) Frictionless flow in a channel, (*b*) a real flow under a deep lighter layer.

'flow force' (the total pressure force plus the momentum flux per unit span) is constant, which gives

$$\tfrac{1}{2}\rho_1(U^2d+g'd^2) = \rho_1(U_2{}^2h+\tfrac{1}{2}g'h^2). \qquad (3.2.10)$$

For consistency of the three relations, Benjamin (1968) showed that

$$U_2{}^2 = 2g'(d-h) = \frac{g'(d^2-h^2)d}{(2d-h)h}, \qquad (3.2.11)$$

whose only non-trivial solution is $h = \frac{1}{2}d$. Thus the only steady, energy conserving flow (this is implied by the use of the Bernoulli condition) is one in which the advancing layer fills half the channel. In this symmetrical case, the Froude number of the approaching flow is subcritical

$$U/(g'd)^{\frac{1}{2}} = \tfrac{1}{2} \qquad (3.2.12)$$

and that of the receding flow supercritical

$$U_2/(g'h)^{\frac{1}{2}} = \sqrt{2}. \qquad (3.2.13)$$

Benjamin has also calculated accurately the shape of the interface; this agrees with an earlier result of von Kármán (1940), who found that the slope of the nose at the stagnation point is 60° to the horizontal.

Many measurements have been made of the flow generated by removing a vertical barrier separating two layers of equal depth and slightly different densities, in channels of various sizes and cross-sections (see Barr 1967). At low flow rates, the Reynolds number must be used explicitly in the interpretation, but for flows on a large enough scale for the direct effects of viscosity to be small, the experiments confirm the near constancy of the nose velocity U over a

considerable length of travel. In completely enclosed wide conduits, the measured velocity is about

$$U = 0.44(g'd)^{\frac{1}{2}}, \tag{3.2.14}$$

not very different from the inviscid value predicted by (3.2.12). In a channel with a free surface, the flow becomes unsymmetrical, the corresponding multiplying constants being 0.47 for the underflow and 0.59 for the overflow.

Lofquist (1960) has made direct measurements of the stress between a single layer flowing along a horizontal plane and a stationary fluid above, and has shown that this is much smaller than the bottom stress. The latter must therefore account for most of the discrepancy between (3.2.12) and (3.2.14), though the interfacial stress can still be important in describing stationary noses (see the next section). Observations of the interface (when one of the layers is dyed) show that it is covered by an irregular pattern of cusped short waves (see fig. 4.13). These have been interpreted either as disturbances due to turbulence generated in each of the layers by the shear at the boundaries, or as a manifestation of a small scale instability of the shear flow at the interface. They will be discussed further in §4.1.4 in the context of interfacial stability, and also in §9.1 when describing the process of mixing at an interface.

3.2.5. *Gravity currents and noses*

When an advancing nose is shallower than half the total depth (as it often is in practice) Benjamin's argument shows that there must be a loss of energy near the front. He has demonstrated further that this energy cannot be carried away in the form of a smooth wave train but must be accompanied by 'breaking'. This is in accord with laboratory observations of gravity currents in deep water (Keulegan 1958) which show that they have 'head' just over twice the depth H of the layer, behind which is a turbulent region and an abrupt drop to the uniform layer behind (see fig. 3.13*b*). The drag associated with the velocity change in the deep layer due to this turbulent wake must be taken into account when considering the force balance on the layer. In no other way can the net force $\frac{1}{2}(\rho_1 - \rho_2)gH^2$

acting in the direction of motion be balanced and a steady state attained.

If one neglects mixing (as we are doing throughout this 'hydraulic' approach), and supposes that the pressure in the 'wake' is hydrostatic, then the velocity of advance U of a nose advancing under a deep fluid can be calculated as follows. The dynamic pressure $\frac{1}{2}\rho_1 U^2$ at the stagnation point must equal the difference in hydrostatic pressure measured at the boundary far upstream and downstream i.e. $g(\rho_1 - \rho_2)H$, so

$$U = 2^{\frac{1}{2}}(g'H)^{\frac{1}{2}}. \qquad (3.2.15)$$

Benjamin (1968) has made the point that these pressures should be compared by taking a circuit passing between the stagnation point and the layer far downstream through the deeper overlying fluid. An earlier argument due to von Kármán (1940), (though giving the same expression for the velocity) is erroneous, since it applied Bernoulli's equation along the interface, an invalid procedure in a dissipating, rotational flow. We note too that the reasoning used by Prandtl (1952, p. 369) is sound only for the initial transient phase of the motion. He equated the dynamic pressures due to the two fluids at the front, neglecting any effects of hydrostatic pressure due to the heavy fluid ejected upwards, and deduced a front velocity half that of the layer behind. As soon as the extra fluid arriving at the nose has fallen back on the underlying layer, a steady state will be achieved in which the nose and layer velocities are nearly equal.

The development of a mixed region of increasing length complicates the argument somewhat, and so does the observed lifting of the stagnation point above the bottom, an effect of bottom friction. Taking the latter into account empirically reduces the multiplying constant in (3.2.15), to give closer agreement with the experimental value of 1.1 suggested by the experiments reported by Keulegan (1958) and Wood (1966). In making this comparison with experiment one must also be careful to allow for the effect of a finite channel depth. When expressed in terms of the layer thickness $H = d - h$, the nose velocity changes monotonically (and almost linearly with H/d) between $2^{-\frac{1}{2}}(g'H)^{\frac{1}{2}}$ for $H = \frac{1}{2}d$, as implied by (3.2.12), and the value (3.2.15) as $H/d \to 0$. Even at $H/d = 0.1$, a common condition in laboratory experiments, the correction can be significant.

The above arguments of course take no account of cross-stream non-uniformities and three dimensional motions, though these have been clearly documented by Simpson (1969) in the laboratory and the atmosphere. (See fig. 3.14, pl. VI.) Something more should be said here too about observations of noses on inclined beds. As the slope is increased the ratio of the front to the layer velocity steadily decreases, and it is down to about 0.7 on a slope of $\frac{1}{20}$. Through the whole of this range of slopes, however, the velocity of the nose can be described using the local density difference and the height D of the head by the relation

$$U = 0.75(g'D)^{\frac{1}{2}}. \tag{3.2.16}$$

A rather more complicated example of the hydraulic approach to 'noses' is provided by studies of the intrusion of a salt wedge far upstream against an opposing fresh water flow. (See Ippen 1966 chapter 11.) Here we consider only a stationary wedge over a flat bottom and a fixed total depth d. The extra factor is that the interfacial stress must now be taken into account explicitly in determining the shape of the interface, and so a momentum equation of the form (3.2.7) is applied to each layer. Assuming again a quadratic dependence of stress on velocity, and that the velocity in the wedge is so small that the bottom stress under it can be neglected compared with that at the interface, one obtains (cf. (3.2.8))

$$(F_1^2 - 1)\frac{\mathrm{d}h_1}{\mathrm{d}x} = C_D F_1^2 \left(\frac{d}{d-h_1}\right), \tag{3.2.17}$$

where $F_1 = U_1/(g'h_1)^{\frac{1}{2}}$ is the internal Froude number of the upper layer. This can clearly be written as a relation involving only h_1 and the distance x (measured from the nose say), using $U_1 h_1 = \text{const.}$

The final step necessary to produce a closed solution is the recognition that a natural control section for the flow of the upper layer occurs where the cross-section increases abruptly either in depth or width (see Wood 1968), for instance at the mouth of an estuary as a river enters the sea. In general, when both layers are moving, the condition here is

$$F_1^2 + F_2^2 = 1. \tag{3.2.18}$$

For a single flowing layer $F = 1$, and no external disturbances can propagate upstream past this point. The integration of (3.2.17) with

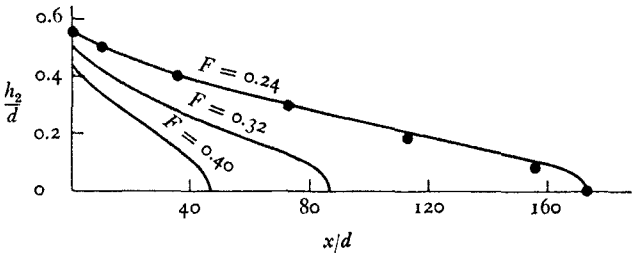

Fig. 3.15. Observed shapes of arrested saline wedges for three fresh water flows (i.e. different internal Froude numbers), with the theoretical points fitted to one of them by Harleman (1961).

boundary conditions applied at the control gives an explicit relation between the initial value of $F = F_0$ say, the depth h_1 and the distance x along the wedge; this is compared with observations due to Keulegan (1957) in fig. 3.15. The total length of the wedge is given by

$$\frac{L}{d} = \frac{1}{4C_D}\left[\tfrac{1}{5}F_0^{-2} - 2 + 3F_0^{\frac{2}{3}} - \tfrac{6}{5}F_0^{\frac{4}{3}}\right]. \qquad (3.2.19)$$

If the mean value of C_D can be regarded as constant, then a knowledge of L for one F_0 allows the evaluation of C_D, which can be used to predict the length of the intrusion for other flow conditions and to calculate the shape of the nose. This method gives results in good agreement with Keulegan's laboratory experiments, though its extension to the full scale phenomenon still involves a good deal of empiricism.

The gradual change in length of intrusion predicted by (3.2.19) should be contrasted with a later result (§6.2.3). When the motion of the bottom layer is taken into account explicitly, there can be a rather rapid transition between a regime of slow flow against the upper current, and a more rapid flow in the same direction. This arises as a result of a change in the rate of mixing (and therefore of the stress) between a turbulent bottom current and the flow outside it, and it is more appropriately discussed in the context of mixing.

3.3. Slow motions in a stratified fluid

3.3.1. *The problem of selective withdrawal*

In many applications (an important example is the design of cooling water intakes for power stations) it is necessary to be able to predict the maximum rate of withdrawal of fluid with desired properties which can be attained before fluid from a different level also begins to flow. The simplest approach to this problem is to use the hydraulic method, and one problem of this kind has already been solved implicitly in §3.2.1. The flow of a layer of heavy fluid through a control section (or over a barrier), where $F = 1$, represents the maximum flowrate for which the lighter fluid is at rest. If fluid is removed at a line sink located on the bottom downstream of the control at any rate less than this, then only the lower fluid will flow out, but if F (based on the mass flux and h_c) rises above a critical value of order unity, then the upper fluid will be drawn in too. Wood (1968, 1970) has shown how this idea can be extended to multi-layer systems flowing through horizontal contractions which act as a control, and has calculated the fluxes in each layer as the total withdrawal rate is increased.

The theory becomes considerably more difficult when a sink discharges from a large body of fluid where there is no clear point of control. Craya (1949) and Huber (1960) considered various cases of sinks in the end wall of a channel, at a different level from the interface between two layers, and proposed methods for calculating the form of the interface as well as the critical condition. Such calculations are at best approximate, and it is often necessary to find the conditions for 'drawdown' experimentally. A fundamental difficulty is that such experiments can never be really steady, because the upstream boundary conditions are altered as the flow continues (see §3.2.2). Nevertheless, practically useful estimates can be made and fig. 3.16 summarizes some of these results for a two-layer system. It is clear on dimensional grounds that, if the orifice width or diameter D is small, the critical condition must always be expressible as $F = F_{\mathrm{crit}}$ where the critical Froude number is defined in terms of g', some flux and the vertical separation h of the sink and interface. For point sinks

$$F_{\mathrm{crit}} = Q_3/g'^{\frac{1}{2}}h^{\frac{5}{2}} \tag{3.3.1}$$

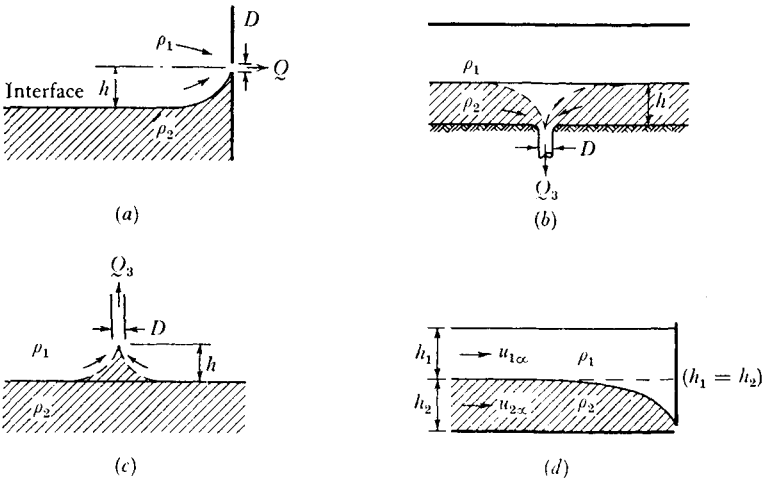

Fig. 3.16. Selective withdrawal of fluid from a two-layer system: critical Froude numbers (as defined in the text) for various boundary conditions. (*a*) Orifice or slot in end wall, $F_{\text{crit}} = 2.6$ (orifice), 1.5 (slot). (*b*) Orifice in bottom, $F_{\text{crit}} = 1.6$. (*c*) Large tube above interface $F_{\text{crit}} = 4.5\,(D/h)^{\frac{1}{2}}$. (*d*) Slot in corner (Huber, theoretical), $F_{\text{crit}} = 1.66$.

and for line sinks $$F_{\text{crit}} = Q_2/g'^{\frac{1}{2}}h^{\frac{3}{2}} \qquad (3.3.2)$$

where Q_3 is a volume flowrate and Q_2 the flux per unit width. This simplification is not always clear from the original papers, where the form in which the results are given puts undue emphasis on D. An explicit dependence on D/h appears in the results of Rouse (1956) shown in fig. 3.16*c* because the orifice diameters ranged up to $D = 10h$.

Similar results hold for continuously stratified fluid, though theoretically they are approached rather differently. Yih (1965, p. 82) used the linear equation (3.1.16) to find a series solution for the flow into a line sink at the end of a channel, with the velocity specified upstream (uniform U in the Boussinesq approximation). He showed that this solution only remains valid provided $F = U/NH$ is sufficiently large, H being the channel depth. For slow flows, when $F < \pi^{-1}$, wavelike solutions also become relevant upstream (cf. §2.3.1) and it is no longer possible to satisfy the boundary conditions at $x = -\infty$, that is, to draw fluid in uniformly from all heights in the channel. The experiments of Debler (1959) have confirmed that

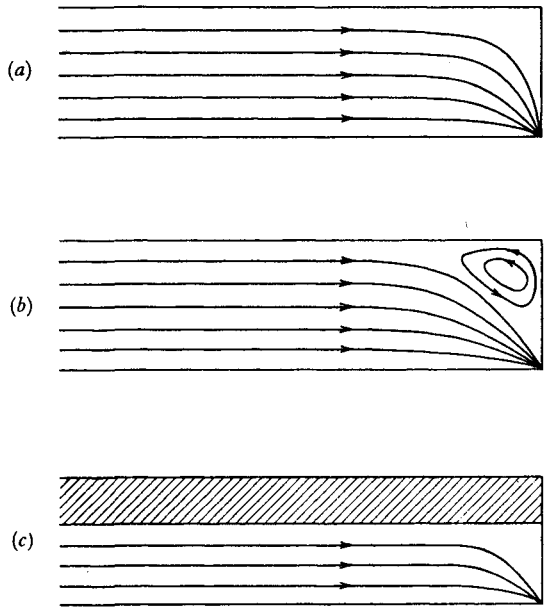

Fig. 3.17. Selective withdrawal from a continuously stratified fluid, (*a*) complete withdrawal, (*b*) the formation of a corner eddy, (*c*) a stagnant upper region.

these solutions give realistic flowpatterns for $F > \pi^{-1}$. As F approaches π^{-1} from above a closed corner eddy appears in the solutions (as shown schematically in fig. 3.17). As remarked earlier in connection with rotors this is not properly described by (3.1.16), but it does (perhaps fortuitously) correspond to what was observed in this range.

For $F < \pi^{-1}$ the fluid is divided into a flowing region and a stagnant layer extending all the way upstream. Debler's results suggest that a similar criterion to (3.3.2) can be used to describe the amount of fluid withdrawn. Defining

$$F_{\text{crit}} = \frac{Q_1}{d_1^2} N^{-1} = \frac{Q_1}{g'^{\frac{1}{2}} d_1^{\frac{3}{2}}} \tag{3.3.3}$$

where Q_1 is the flux per unit width, d_1 is the depth of the flowing layer far from the source and g' is based on the density difference across d_1, the experiments correspond to a value of $F_{\text{crit}} = 0.25$. It turns out to be a good general rule for all kinds of slow flows that this

internal Froude number, based on the properties of the flowing layer (or each of the layers, if there is more than one), lies between $\frac{1}{4}$ and $\frac{1}{3}$, the lower values probably being due to viscous effects which have so far been neglected here. Yih (1965, p. 90) has shown how the formation of a stagnant region can be postponed to smaller F by inserting an obstacle near the sink (whose form was calculated by an indirect method, using an array of singularities and choosing a closed streamline). At even lower F blocking must inevitably occur, when a layer of fluid at the bottom of the channel cannot flow over the barrier.

3.3.2. *Blocking ahead of an obstacle*

It is clear both from the lee wave experiments described in §3.1.4 and the sink flows just discussed that it is not profitable to treat slow flows in a density gradient, for which $F \ll 1$, using a steady model and fixed upstream boundary conditions. Now it is appropriate to recall the result quoted in §2.2.2; in the limit $F \to 0$, a two-dimensional body in steady horizontal motion will carry along with it a plug of fluid bounded by tangents above and below it and extending to infinity both up and down stream. What is observed experimentally (see fig. 3.18 pl. VII) just after such a body is set into slow motion is not so simple, however. In addition to a plug of finite length directly ahead of the body, an array of alternating jets develops at other horizontal levels. These jets become more numerous as F is reduced, and they all propagate upstream in time, altering the approaching flow. All of these results can be reconciled provided the flow is treated as *time-dependent*, and the approach to a steady state is examined as an initial value problem.

Using a model of this kind Trustrum (1964) obtained solutions which contain features resembling Long's and Debler's observations (and also some analogous results for rotating fluids, which will not be described here). She assumed a steady inviscid flow with constant U and linear density gradient, into which at $t = 0$, $x = 0$, a disturbance (in the form of a source–sink distribution) is inserted. The governing equations in this essentially linear theory were derived using the Boussinesq assumption, and also one of the Oseen type in which the perturbation velocity is ignored in the

convective terms. With the convention (to be used also in §3.3.3) that the mean flow is in the negative x-direction, her solutions as $t \to \infty$ are periodic in both x and z for $x < 0$ (i.e. for appropriate boundary conditions they describe lee waves downstream), whereas the upstream solutions are periodic in z and independent of x, and therefore describe one-dimensional flows extending to $x = +\infty$ (the columnar modes). The magnitude of both parts of the flow is proportional to the strength of the source–sink distribution, as in Yih's solutions, but the new terms (those independent of x) were previously excluded by the initial assumption of uniform upstream velocity. When the method is applied to sink flows, realistic looking closed streamlines are obtained. The approximations are strictly valid only far from the sink, however, and even there the predicted perturbations upstream are finite and not small, so the basic assumption leading to the linearized theory becomes questionable again.

Another approach to the time-dependent problem was made by Bretherton (1967) who examined the development of the flow in terms of waves propagating away from the body. (His analysis too was carried out for inertial waves in a rotating fluid, i.e. for a 'Taylor column', but the translation of the results to the case of plane gravity waves in a stratified fluid is immediate.†) His physical interpretation is as follows. If a cylindrical body is rapidly accelerated from rest to a small horizontal velocity, gravity waves will be generated, which spread out in all directions. Far from the body, the larger scale waves arrive first, since for any angle of propagation the group velocity depends inversely on k (2.2.11), and a broad velocity profile is at first produced (fig. 3.19*a*). In the region ahead of the body the waves have zero frequency but finite group velocity relative to the body. As more energy is put into the fluid, the length of the steady flow region increases at a finite rate comparable with the group velocity of waves whose half wavelength is equal to the diameter of the obstacle.

Regions of larger velocity gradients can build up later as the slower shorter waves arrive, and fig. 3.19*b* shows the velocity profile

† The analogy has been important in the development of the subject, though it will not be pursued in detail here. For a full discussion see Veronis (1967), which is referred to in another context on p. 243.

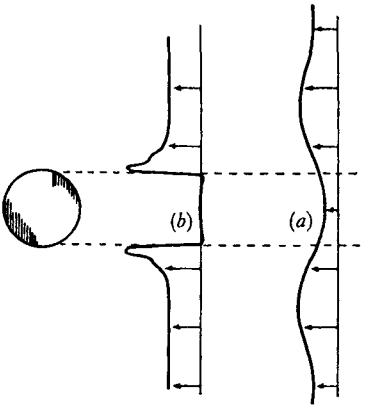

Fig. 3.19. The development of a blocked flow far from a cylinder moved slowly in a horizontal direction through a stratified fluid. (*a*) Broad velocity profile due to the first long waves. (*b*) Plug flow produced much later as the slower short waves arrive. (From Bretherton 1967.)

at a later time; the central plug flow is now nearly at rest relative to the body. This profile was calculated by superposing the velocities due to all the waves which had arrived at the time of interest (which implies the restriction of infinitesimal motion and hence linear equations). Very near the surface of the body a singularity tends to develop because of the cumulative effect of very small scale waves which have not had time to propagate away. Bretherton went on to discuss the effect of a small viscosity on his inviscid solutions. He argued that this could be treated separately from the problem of generation and propagation, and that each wave component will decay exponentially at a rate which increases as the wavelength decreases. The singularities will be removed in a real fluid because the shortest waves are rapidly damped, but the longest waves are little affected. Ultimately a steady state is predicted in which the 'blocked' regions are of finite length.

Whatever detailed model is used to describe these slow flows it is clear that an inviscid solution must become physically unrealistic in two regions. Very near an obstacle a viscous boundary layer must dominate, and at large distances viscosity must eventually cause all the disturbances to die away. Problems in which viscous (and also diffusive) terms have been taken explicitly into account are discussed in the following sections.

3.3.3. *Upstream wakes and boundary layers*

Martin and Long (1968) have given a careful derivation of the relevant equations (to which reference should be made for the details), but the essential points can be made simply from first principles. Consider a steady motion in which fluid particles preserve their identity and properties (i.e. there is no diffusion), and in which viscous and buoyancy forces are dominant. One can then neglect the time-dependent and inertial terms on the left of (1.3.3) to obtain the component Navier–Stokes equations

$$\left.\begin{aligned} 0 &= -\frac{\partial p'}{\partial x} + \nu\nabla^2 u, \\ 0 &= -\frac{\partial p'}{\partial z} - g\frac{\rho'}{\rho_0} + \nu\nabla^2 w, \end{aligned}\right\} \tag{3.3.4}$$

where p' and ρ' are the perturbation pressure and density (cf. (1.3.4)). Now eliminating the pressure by cross-differentiation, and at the same time using a boundary layer type of approximation to neglect the higher x derivatives, gives

$$\frac{g}{\rho_0}\frac{\partial \rho'}{\partial x} = -\nu\frac{\partial^4 \psi}{\partial z^4}, \tag{3.3.5}$$

where ψ is the streamfunction defined as in §3.1.3 by $u = \partial\psi/\partial z$, $w = -\partial\psi/\partial x$. This last assumption is justified by the fact that the flows of interest (as in the inviscid case), are elongated horizontally, and have much smaller variations in the x- than in the z-direction.

Again the discussion is simplified if one assumes that far upstream there is a uniform flow, say in the negative x-direction, with a linear density gradient (cf. §3.1.3), i.e.

$$\psi = -U_0 z, \quad g\rho'/\rho_0 = -N^2 z.$$

Since without diffusion ρ' must be constant along streamlines, combining these two gives a relation between ψ and ρ' which is valid even when the flow is disturbed by the introduction of a thin obstacle:

$$\frac{g\rho'}{\rho_0} = \frac{N^2}{U_0}\psi. \tag{3.3.6}$$

Substituting this in (3.3.5) gives a single equation for ψ

$$\frac{\partial^4\psi}{\partial z^4} + \beta\frac{\partial\psi}{\partial x} = 0, \tag{3.3.7}$$

where $\beta = N^2/U_0\nu$ has the dimensions of (length)$^{-3}$. If this is made non-dimensional using a lengthscale L (say the length of the body or the distance along it) so that $x = Lx_1$, $z = Lz_1$, then

$$\frac{\partial^4\psi_1}{\partial z_1^4} + \beta_1\frac{\partial\psi_1}{\partial x_1} = 0. \tag{3.3.8}$$

Here $\beta_1 = N^2L^3/U_0\nu$ is the ratio of buoyancy to viscous forces, which can be written in the form of a Richardson number Ri_0 times a Reynolds number Re, where $Ri_0 = N^2L^2/U_0^2$, $Re = U_0L/\nu$. Martin (1966) has shown further that the terms neglected in arriving at (3.3.7) are of order $(Re/Ri)^{\frac{1}{2}} = Re\,\beta_1^{-\frac{1}{2}}$ if $Re \gtrsim 1$; this latter ratio is therefore a measure of the importance of higher order inertia terms relative to those retained. We also note here for later reference his result that the neglect of diffusion is justified provided

$$\kappa Ri^{\frac{1}{2}}/\nu Re^{\frac{1}{2}} \ll 1,$$

where κ is the molecular diffusivity of the property causing the density variations.

The parabolic nature of (3.3.8) implies that, just as in the ordinary one-dimensional diffusion equation in which time is analogous to the variable x_1, boundary conditions imposed upstream of a given flow section (cf. those imposed at future times) cannot influence the flow there. This approximation therefore means that in the region behind a body there is no way in which its presence can be felt by the fluid. Ahead of the body there will, however, be an *upstream wake*, whose form can be calculated from (3.3.7) using the boundary conditions imposed on the body and upstream (in the positive x_1-direction). This asymmetry in the behaviour can also be deduced using a physical argument based on vorticity; only upstream of a body is the vorticity generated by buoyancy in the opposite sense to that generated by viscosity, so that a balance between the two becomes possible.†

† It is of course the restriction to very slow motions which has eliminated the possibility of the more familiar kind of wake, whose properties in the limit of *large* velocity will be treated in chapter 5.

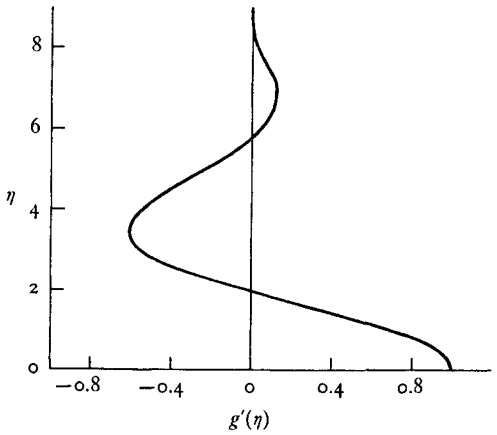

Fig. 3.20. The horizontal velocity profile in an upstream wake. (From Martin and Long 1968.)

Two special solutions of (3.3.7) with different boundary conditions are of interest here. Far upstream of the body the form of the solution does not depend on the details of the flow around it, but only on the drag D or the momentum defect flux

$$J = \frac{D}{\rho} = \int_{-\infty}^{\infty} p' \mathrm{d}z \tag{3.3.9}$$

which is constant at all sections upstream. Long (1959) showed that, by choosing a certain combination of powers of x and z as a new independent variable, (3.3.7) with the condition (3.3.9) can be reduced to an ordinary differential equation, i.e. he found a similarity solution which can be written as

$$\psi = \frac{J}{\nu}(\beta x)^{-\frac{1}{4}} g(\eta), \tag{3.3.10}$$

where

$$\eta = z\left(\frac{x}{\beta}\right)^{-\frac{1}{4}}. \tag{3.3.11}$$

The substitution of these expressions into (3.3.7) gives the equation for the non-dimensional function $g(\eta)$ (dashes denoting derivatives),

$$4g^{\mathrm{iv}} - \eta g' - 2g = 0, \tag{3.3.12}$$

which was solved numerically by Long to obtain (for example) the horizontal velocity profile reproduced in fig. 3.20. Qualitatively this agrees with the alternating jet structure which is observed, but

Martin and Long (1968) showed that it is difficult to go far enough upstream to make the direct effect of a body negligible and obtain a quantitative experimental check.

Pao (1968*a*) also produced comparable solutions for the upstream wake, and carried out experiments (see fig. 3.21 pl. VII) covering a range of values of Re/Ri_0 between 0.2 and 10. At the higher values of this ratio (as inertia effects became increasingly important) he showed that the wake becomes weaker but that successive velocity maxima spread out further vertically. These features are predicted by the theory of Janowitz (1968), who, instead of neglecting inertial terms entirely, linearized the equations of motion using the Oseen approximation (compare §3.3.2). He also showed that decaying lee waves can exist downstream, which attenuate more slowly as the speed of the body increases.

Graebel (1969) has extended the theory based on (3.3.7) to include bodies with a finite vertical thickness $2b$, taking b as the lengthscale in β_1 instead of L. He showed that the blocked region upstream has a length of order β_1, and that here viscosity must act to raise a fluid particle against gravity so that it can pass the body, while behind gravity is the principal controlling factor. The resulting difference in pressure distribution, nearly constant immediately upstream in the stagnant region and varying hydrostatically downstream as in the original undisturbed fluid, dominates the drag, which can be expressed to this approximation as

$$D = \rho J = \tfrac{2}{3} g b^3 \left| \frac{\mathrm{d}\rho}{\mathrm{d}z} \right|, \tag{3.3.13}$$

independent of both viscosity and speed (though of course the existence of viscosity and some motion is essential to establish the pressure distribution).

A second similarity solution of (3.3.7) has been found to describe the motion immediately over a thin plate (i.e. the upstream boundary layer). Taking the plate to be semi-infinite $0 \leqslant x \leqslant \infty$ (and the origin therefore at the back of the plate), the solution corresponding to boundary conditions of no slip at the surface and small disturbances at large z is

$$\psi = U_0 \left(\frac{x}{\beta}\right)^{\frac{1}{4}} f(\eta), \tag{3.3.14}$$

with η again defined by (3.3.11). This represents a boundary layer

which grows upstream from the back of the plate, and it is also applicable to finite plates because of the property that conditions upstream cannot affect the flow at any given section. Substitution of (3.3.14) into (3.3.7) gives an ordinary differential equation for $f(\eta)$ comparable to (3.3.12) whose numerical solution gives the horizontal velocity profile.

Several of the predictions of this theory have been verified in a careful series of experiments carried out by Martin (1966), using streak photography of aluminium particles suspended in a large channel of stratified salt water. He measured the heights of the first two stagnation surfaces (i.e. the positions where the flow was moving with the free stream velocity, in a cordinate system moving with the plate), and obtained excellent quantitative agreement with (3.3.14) in the region of its validity. He also clearly demonstrated the upstream growth of the boundary layer from the back of the plate. (See fig. 3.22 pl. VII.) The two conditions mentioned following (3.3.8) do, however, place severe (and opposing) restrictions on the range of applicability of (3.3.14). Inertia becomes important at large velocities and very close to the rear of the plate. More serious is the neglect of diffusion, which becomes important near the plate at *low* velocities, because of the wrong boundary condition imposed on the salinity field there. A diffusive boundary layer grows from the front of the plate, and this can become thick enough at the rear edge to have a visible effect on the flow. For these reasons, the experiments are limited in practice to velocities of about 1 mm/s with very slowly diffusing substances, and it is impossible to get a range of conditions where both these effects are negligible if a temperature gradient in water is used to produce the density variation.

3.3.4. *Viscous diffusive flows*

When diffusion is introduced into the problem, it is no longer permissible to use the assumption that ρ' is a function of ψ alone, which led to (3.3.6) and to the elimination of ρ' from (3.3.5). Instead, one must add to (3.3.4) (or the more general form of these which includes inertial effects) a diffusion equation

$$u\frac{\partial \rho'}{\partial x}+w\frac{\partial \rho'}{\partial z}=\kappa\frac{\partial^2 \rho'}{\partial z^2}, \qquad (3.3.15)$$

where κ is the diffusivity of the substance producing the density gradient. Equations (3.3.5) and (3.3.15) must now be treated as a coupled pair, from which ρ' can be eliminated to give a single sixth-order equation for ψ. With the extra assumptions that the density gradient is linear and that perturbations to this gradient can be neglected (and again making the boundary layer assumption and taking the velocity to be small), (3.3.15) becomes

$$N^2 \frac{\partial \psi}{\partial x} = \frac{g\kappa}{\rho_0} \frac{\partial^2 \rho'}{\partial z^2}. \tag{3.3.16}$$

Eliminating ρ' from (3.3.5) and (3.3.16) gives

$$\frac{\partial^6 \psi}{\partial z^6} + B \frac{\partial^2 \psi}{\partial x^2} = 0, \tag{3.3.17}$$

where $B = N^2/\kappa\nu$.

In all problems where diffusion replaces inertia as a significant parameter (and buoyancy and viscosity remain important), the combination B, having dimensions of (length)$^{-4}$, always emerges, and replaces the β which appeared in (3.3.7). The non-dimensional form of this parameter, $B_1 = L^4 B$, where L is a characteristic horizontal lengthscale of the problem, is a Rayleigh number (see chapter 7). Koh (1966) showed how higher order approximations (in which (3.3.17) corresponds to the zeroth order term) can be developed using an expansion technique. The appropriate expansion parameter is equivalent to $Pe \cdot B_1^{-\frac{1}{4}}$ (where $Pe = Q/\kappa$ is a Péclet number based on the volume flux per unit width Q). This combination is therefore a measure of the importance of inertia relative to the terms retained and its smallness ensures the adequacy of (3.3.17), in which B (or B_1) alone determines the behaviour. (Compare with the different roles of $Re \cdot \beta_1^{-\frac{1}{2}}$ and β_1 discussed in the preceding section after (3.3.8).)

In just the same way as before, similarity solutions of (3.3.17) can be found for wakes and boundary layers by imposing appropriate boundary conditions.† It should be noted immediately, however, that the governing equations are no longer parabolic, and so the

† All the solutions considered here are for infinitely large regions; the extra problems introduced by vertical boundaries are discussed by Foster and Saffman (1970).

solutions for the wake which include diffusion are symmetric, valid downstream as well as upstream of the body. Long (1962) found the stream function for the wake far from a body, which can be expressed in terms of the drag ρJ, the parameter B and the geometry as

$$\psi = \frac{J}{\nu}(Bx)^{-\frac{1}{3}} g_1(\gamma) \tag{3.3.18}$$

with

$$\gamma = B^{\frac{1}{6}} z / x^{\frac{1}{3}}. \tag{3.3.19}$$

(Compare with the viscous, non-diffusive case (3.3.10), and (3.3.11) in which there was a different dependence on x.) The function $g_1(\gamma)$, obtained by numerical integration of the resulting ordinary differential equation, is very similar to that for $g(\eta)$ (reproduced in fig. 3.20) and will not be drawn here.

The diffusive boundary layer, which grows from the *front* of a thin plate (now taken as the origin), is described by

$$\psi = -U_0 x^{\frac{1}{3}} B^{-\frac{1}{6}} f_1(\gamma) \tag{3.3.20}$$

with γ defined by (3.3.19). Again the form of $f_1(\gamma)$ is not very different from that of $f(\eta)$ in (3.3.14). The ratio of the coefficients in (3.3.20) and (3.3.14), at a fixed value of x, can be used to assess the importance of diffusion; this agrees with the criterion stated in the previous section.

A third problem in which diffusion matters as well as viscosity and buoyancy is that of the very slow withdrawal of a continuously stratified fluid from a two-dimensional slit placed at the origin (Koh 1966). In this case the stream function must be everywhere proportional to the volume flux per unit width Q, and to the same order of approximation as before

$$\psi = -Q f_0(\gamma), \tag{3.3.21}$$

where f_0 is another non-dimensional function of the same similarity variable $\gamma = B^{\frac{1}{6}} z / x^{\frac{1}{3}}$. The fluid removed will come from a confined region near $z = 0$ (like an internal boundary layer), and the horizontal velocity has a sharp peak at this level. The shape of the withdrawal layer (see fig. 3.23) can be deduced from the form of γ, using the numerical solution for f_0 only to find the numerical con-

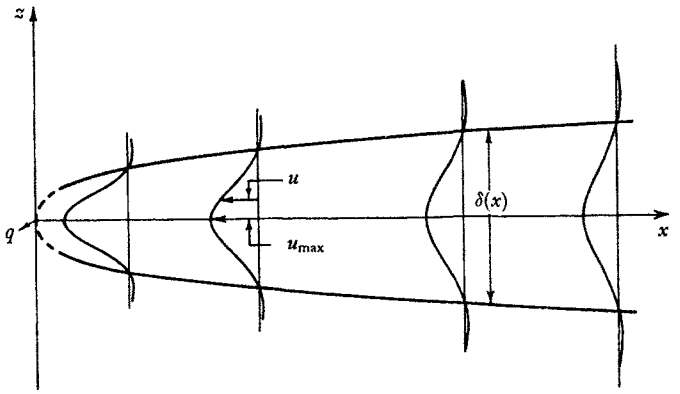

Fig. 3.23. Viscous stratified flow towards a line sink. Calculated form of the withdrawal layer. (From Koh 1966.)

stant. Thus the edge of this region corresponds to the value of γ where $f_0(\gamma) = 0$ i.e. to $B^{\frac{1}{3}}z/x^{\frac{1}{3}} = \gamma_\delta = \text{constant}$.

Koh (1966) evaluated the constant by assuming that this theory remains valid right to the origin, and predicted that

$$\delta(x) = 7.14x^{\frac{1}{3}}B^{-\frac{1}{3}}. \qquad (3.3.22)$$

Later work (Imberger 1972) has shown, however, that the observed thicknesses are consistently greater than this, and in agreement with a theory which takes inertial forces properly into account. Near a strong sink the inviscid theory discussed in §3.3.1 will apply to a layer of uniform depth in which inertial effects matter, but at large distances viscosity and diffusion eventually dominate, and the layer must spread out further vertically (by an amount which is given approximately by (3.3.22)). In some practical situations, for example in reservoirs, $Pe \cdot B_1^{-\frac{1}{3}}$ may never be small enough for inertia to be neglected even at the far end of the region of interest.

Vertical profiles of horizontal velocity were also predicted by Koh, using the numerical solutions for f_0 to calculate $u = \partial\psi/\partial z$ from (3.3.21). These were compared with measurements in a large channel of water stratified with either temperature or salinity, by recording photographically the distortion of vertical streaks of dye as fluid was withdrawn steadily at one end. The measured shapes were in good agreement with theory at all positions along the tank, though the

magnitudes differed from the simple prediction based on the buoyancy–diffusion theory. This was attributed to the neglect of inertial effects, but we should emphasize again the fundamental problem of time dependence, which will be just as serious for viscous as for inviscid flows (see §3.3.1). Experiments of this kind cannot achieve a steady state, though in the absence of a simple alternative they are interpreted using relations like (3.3.22) which are based on this assumption.